

# Estimation of IMFP except for a constant factor using only XPS background-optimized peak intensities and cross sections

Masatoshi Jo,\*

National Metrology Institute of Japan, AIST

AIST Tsukuba Central 5, 1-1-1 Higashi, Tsukuba, Ibaraki 305-8565, Japan

\* m-jo@aist.go.jp

(Received : November 30, 2013; Accepted : January 30, 2014)

A method for estimation of inelastic mean-free path (IMFP or  $\lambda$ ) of an unknown material except for an arbitrary proportionality constant  $c$ , i.e.  $\lambda_0(E)$  in  $\lambda(E)=c\lambda_0(E)$ , where  $E$  is the electron kinetic energy, has been proposed through iteration of background optimization on an XPS spectrum. The dependence of the  $i$ -th core peak intensity  $p_i$  on its energy  $E_i$  given by background optimization is proportional to the product of theoretical photoexcitation cross sections  $\sigma_i$  and the asymmetry factor  $a_i$  after analyzer transmission correction. Therefore, any non-parallel behavior between  $p_i$  and  $(\sigma_i \cdot a_i)$  is ascribed to  $\lambda(E)$ . This enables the estimation of  $\lambda_0(E)$  using  $p_i$  and  $(\sigma_i \cdot a_i)$ , by assuming the initial  $\lambda$  to be constant, and then repeating background optimization and  $\lambda$  update. Between 700 and 1500 eV kinetic energy (KE) for Au metal, where  $\lambda$  by TPP [Tanuma et al, Surf. Interface Anal., 43,689(2011)], denoted as  $\lambda_{\text{TPP}}$ , is known to be well approximated by a straight line,  $\lambda$  converges to  $\lambda_{\text{TPP}}$  within 2.4 % if  $c$  is chosen so that both values coincide at 800 eV. This is remarkably satisfactory because only relative peak intensities are involved in a usual practical analysis and because what is requested for surface analysis is to analyze the sample whose properties including  $\lambda$  are yet to be known.

## 1. Introduction

Surface analysts working for practical purposes must deal with almost all kinds of materials whose surfaces attract attention. Since these surfaces are usually vulnerable, interpretation of two different measurements should always be treated with greatest care. In the first place, the necessity of surface analysis comes from the fact that the region is too small to access by usual macroscopic methods, or is not the same as imagined from idealized cut of the bulk material as a result of all the events before (and during) the measurement. Therefore, the problem today's surface analysis must answer is the one very specific to the current particular unknown specimen. As for inelastic mean free path (IMFP or  $\lambda$ ), it follows that  *$\lambda$  cannot be determined completely until its various material-dependent parameters such as atomic density, plasmon energy, band gap, etc. are determined, whereas it is also recognized that  $\lambda$  is one of essential parameters to perform surface analysis by electron spectroscopy and is expected to be given before the analysis.* In the present

report, a way to estimate relative kinetic-energy dependence of  $\lambda$  without referring to an unknown composition, which is practically suitable to usual analysis, is proposed in order to circumvent the self-contradiction posed above, through an analysis of XPS spectrum using an iterated background optimization method.

## 2. Method's Detail

It is noted the terminology has been changed from the previous report [1] for clearer understanding. This section describes how unknown  $\lambda$  is estimated using the background optimization method. The method comprises a number of the same background optimization jobs associated with different constraints in order to cover the possible physical situations in the problem as a whole. Detailed algorithm of the individual job is already described in ref.[1].

### 2.1 The outline of background optimization

The principle of background subtraction algorithm

based on Tougaard's formula [2] is summarized in Fig. 1.

In Fig. 1, the inelastic background  $g(E)$  is given by integrating the transmission-corrected spectrum  $J_0(E)$  multiplied by  $K^0$  that expresses the energy loss probability. Subtracting  $g$  from  $J_0$  gives the primary excitation spectrum  $J$ . The background optimization method mainly optimizes the *shape* of  $K^0$  in order to satisfy the constraints imposed on  $P_1$ ,  $P_2$  and  $T$ , which correspond to the areas of *Peak(1)*, *Peak(2)* and the absolute area of *Tail*, respectively, as summarized in Fig.1 and Table 1. *Peak* is the generalized interval including several distinct "ordinary" peaks where considerable intensity is expected. *Tail* is the interval outside *Peak*, where intensity is low.  $i$ -th *Peak* is denoted as *Peak(i)*.  $P_i$  and  $T$  are their integrals, respectively, though  $T$  is evaluated by the absolute value.

The objective function of the present optimization problem is given by  $F(K)$  in Table 1, where the

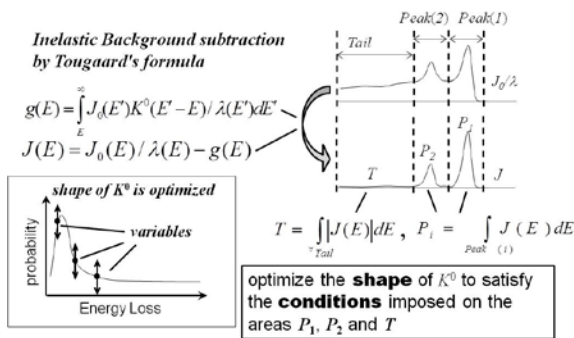


Fig. 1 Background Optimization using Tougaard's Formula

Table 1 Physical meanings of objective function and constraints.;  $P_i$ ,  $T$  : intensities of *Peaks* and *Tail*,  $A_0$  : normalization factor for intensities ;  $P^U$ ,  $P^L, T^U$  : upper and lower boundaries of normalized intensities  $P_i/A_0$ , and  $T/A_0$

usage as	expression	meanings
objective function	$F(K) = \left  \frac{P_2}{P_1} - \frac{P_1}{P_2} \right  \rightarrow 0$	$A_1:A_2 = S:1$ intensity is stable around $S$
constraints	$c_{p,l}^i(K) = \frac{P_i}{A_0} - P^L \geq 0$	normalized intensity $P_i/A_0$ is larger than $P^L$
	$c_{p,u}^i(K) = P^U - \frac{P_i}{A_0} \geq 0$	normalized intensity $P_i/A_0$ is smaller than $P^U$
	$c_{t,u}(K) = T^U - \frac{T}{A_0} \geq 0$	normalized intensity $T/A_0$ is smaller than $T^U$
	$c_{neg}(K) = \int \min(0, J(E))dE = 0$	no negative intensity allowed

expression "(K)" denotes the dependence on the whole shape of  $K^0$ . The optimization condition  $F(K)=0$  represents the fact that the intensity ratio of two *Peaks* is equal to that predicted for  $J$ , and stationary around optimized  $K^0$ , because all the inelastic effects originating

from  $K^0$  are removed from  $J$  and contained in  $g$ .

Three out of the four constraints,  $c_{p,U}^i$ ,  $c_{p,L}^i$  and  $c_{T,U}$ , assert that  $P_1$ ,  $P_2$  and  $T$  must be bounded by Upper and Lower limits of Peak and Upper limit of Tail, denoted as  $P^U$ ,  $P^L$ , and  $T^U$ , respectively. The last one  $c_{neg}$  states that  $J$  must not become negative for any real data.

$A_0$  in the constraints is a common scaling factor introduced for convenience. In the present study,  $A_0$  is taken as an area of one of the *Peaks* calculated using simpler method, such as the Shirley background.

In addition to the constants in the inequalities, LSStep, which works in the original optimization routine SQP [3], is also used. This defines an upper limit of the radius in a search for the next iteration point in each single job.

## 2.2 The Batched Background Optimization

The above four constants,  $P^U$ ,  $P^L$ ,  $T^U$  and LSStep defines an optimization job. It is obvious that only very limited combinations of them would give a reasonable solution, and otherwise not. In order to select out the reasonable solution, a series of jobs with variations of these constants is constituted. This is denoted as a "batch calculation". The number of jobs, which is characterized by the combination of the above four constants, is on the order of 100. Note that the number of combinations explodes easily.

A judgment criterion to decide whether the solution is reasonable or not is as follows. If Tougaard's universal function is used, the background-subtracted spectrum still shows a blowup towards lower kinetic energy due to secondary electron emission. The base line of the spectrum obeys a power law of kinetic energy,  $E^{-k}$ , where  $k \sim 2$  typically. Therefore, it is reasonable to assume this functional form continues to higher energy but is not always seen due to incomplete tuning of  $K$ . The criterion is thus set as follows. Compute  $k$  using the region at the lower energy side where  $E^{-k}$  is dominant and then extend the line towards higher energy where dominant peaks are observed. Among the results after further removal of this particular base line from each  $J$ , the one with least inappropriateness, i.e., the least negative minimum and simultaneously least unnecessary intensity, is selected. By inspecting the selected spectrum, the range of constants for the appropriate combination is narrowed down. Repeating these processes several times by updating the constraints, the result converges to a single

state, which indeed looks like a very good background subtraction as will be shown in Fig. 2b. In the final result, the relative core peak intensities are in good agreement with cross sections calculated by Scofield [4] and asymmetry factors [5] as will be shown in Table 2.

Table 2 Core peak intensities of the present result and  $(\sigma \cdot a)$  [4,5], all normalized by the values of 4f.

Name	present result	$\sigma \cdot a$
5p3/2	0.062	0.068
5p1/2	0.025	0.029
4f	1	1
4d	1.21	1.17
4p3/2	0.37	0.36
4p1/2	0.13	0.13
4s	0.10	0.12

### 2.3 Estimation of unknown $\lambda$

In the present analysis, transmission-corrected data are required to proceed. For such data, the factors affecting the peak intensities remain only in  $\lambda$  and/or in the background optimization method itself. Therefore, if both  $\lambda$  and the determined background are correct, the peak intensity should be proportional to their theoretical value that is expressed by the photoionization cross section  $\sigma$  and the angular asymmetry factor  $a$ . The factor  $a$  taking into account elastic scattering for the  $i$ -th peak is written as

$$a_i = 1 - \beta_{i,\text{eff}} \cdot \frac{3\cos^2\phi - 1}{4}$$

where  $\beta_{i,\text{eff}}$  is the asymmetry parameter calculated by Jablonski [5].

On the contrary, if the intensity variation for each core level is not parallel with the result from background optimization, the reason is ascribed to  $\lambda$ . Suppose that  $p_i$

is the intensity by using  $\lambda_i(E)$  as a tentative IMFP value and  $p_c$  the one using the correct IMFP  $\lambda_c$ . Then it is obvious that  $p_i \propto (\lambda_c / \lambda_i) p_c$ . Since  $p_c \propto (\sigma \cdot a)$ , then  $p_i / (\sigma \cdot a) \propto \lambda_c / \lambda_i$ , and finally  $\lambda_c \propto p_i / (\sigma \cdot a)$  if  $\lambda_i$  is set to be constant.

The final expression above leads to a way to estimate the unknown  $\lambda$  as follows.

(a) Assume that  $\lambda_i = \Lambda = \text{const.}$

(b) Subtract inelastic background by the batched background optimization method, and then the  $E^{-k}$  baseline described above. Examination of this process gives  $K^0$ .

(c) Calculate  $p_i$ 's using the obtained  $K^0$  and the constant  $\lambda = \Lambda$ .

(d) Substitute  $\lambda_i$  by  $p_i / (\sigma_i a_i)$  where  $\lambda_i$  is the value at energy  $E_i$  and  $a_i$  is the asymmetry factor [5] mentioned above.

(e) Update entire  $\lambda$  as a straight line fitted to  $\lambda_i$ 's and return to (b).

This procedure will converge because the substitution in (d) reassigns the same  $\lambda_i$  for correct values. The reason that a straight line is used in step (e) is because most of the known IMFP's are monotonically increasing and featureless above  $E > 100$  eV and they are properly approximated by straight lines fitted to the points at  $E_i$ 's, except for the region of very low kinetic energy where a rapid increase towards lower energies appears, or at higher energies where the deviation from a straight line is significant.

It is noted that  $a_i$  can be omitted by using the instruments configured in the so-called magic-angle geometry, i.e.  $\phi = 54.7^\circ$ , where the coefficient of  $\beta_{i,\text{eff}}$  vanishes. In this case the analysis can be done without

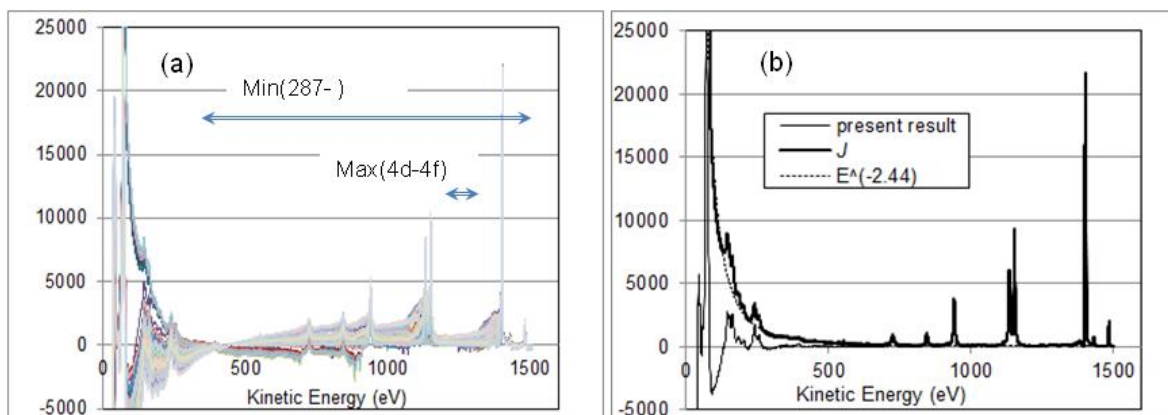


Fig. 2 Results all and selected in the last stage. (a) All results. Horizontal arrows indicate the intervals for selection. (b) selected  $J$ , power-law baseline  $E^{-k}$  with  $k=2.44$ , and baseline-removed spectrum.

referring to the solid-state information.

It is also noted that, since the background optimization is designed to deal with only the ratio of areas calculated from  $J$ , the magnitudes of the constant factor  $c$  in  $\lambda$  and the tentative constant  $\Lambda$  have no effects due to automatic cancellation.

### 3. Experimental and Analysis Conditions

A wide-scan Au XPS spectrum with 0.5 eV step taken by PHI-1600c spectrometer with monochromatic Al  $K\alpha$  source is used, after transmission correction according to the procedure by Tanaka [6]. The angle between the X-ray and analyzer directions is  $70^\circ$ . The analyzer direction is normal to the surface. The 4d peak is used for  $A_0$ . The pair of Peaks employed in the objective function  $F$  is 4d and 4f.  $\lambda_0$  is calculated as a straight line fitting to the ratios at seven core peaks, 5p $_{3/2}$ , 5p $_{1/2}$ , 5d(3/2+5/2), 4f(7/2+5/2), 4p $_{3/2}$ , 4p $_{1/2}$  and 4s. The initial shape of  $K^0$  is given by the shape coinciding with the Tougaard's 2-parameter universal function with  $B=3047$  eV $^2$  and  $C=1100$  eV $^2$  [2], which had been chosen only for convenience in the previous studies [1] (shown in Fig.3). For the present case, it was possible to update  $\lambda$  without changing the batch condition. Two intervals for classification of the result are defined as shown in Fig. 2a. A region shallower than 1200 eV binding energy (BE) (=287 eV kinetic energy (KE)), denoted as Min(287 -), where all the core peaks are situated is used for the calculation of the minimum that suggests over-subtraction if it is less than zero, and another region between 286.5 and 214 eV BE, i.e. between the 4d and 4f peaks, denoted as Max(4d-4f), for the maximum that

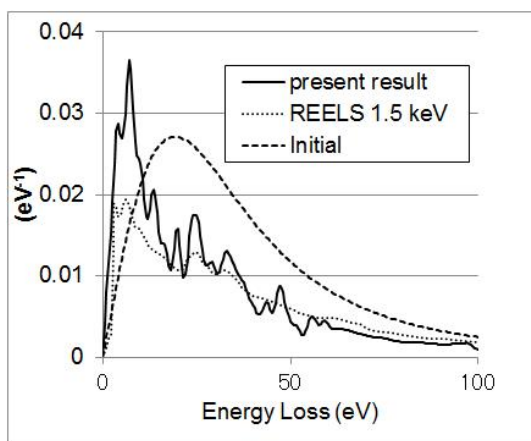


Fig. 3 Initial and final forms of  $K^0$ , together with  $\lambda * K$  by REELS experiment [7].

suggests insufficient subtraction if it is considerably large. Sorting by these values makes it possible to select the most plausible result. Typical computation time per one job is 1-2 minutes. The present batch comprising 144 jobs takes 2-3 hours. The exponent  $k$  for the  $E^{-k}$  baseline is calculated using two intensities at 53.2 and 442.2 eV KE of  $J$ , the primary excitation spectrum.

### 4. Results and discussion

#### 4.1 Job Selection and the selected Result

Starting with  $\lambda = 10 \text{ \AA}$  (=constant), four trials were made to reach the present result. Fig.2a and 2b show the results of all jobs and the one selected from the last stage, respectively. The features in the preceding stages look similar, except for the different peak ratios. Two intervals for the selection criteria defined above are also shown in Fig.2a. The selected  $J$  is shown in Fig.2b. It was found that the "not good" spectra usually include both negative and excessive parts. Therefore, the sort by Min partially works as sort by Max, and vice versa. Fig.2b also shows the  $E^{-2.44}$  baseline and the baseline-subtracted region where core peaks are observed. On the contrary, the agreement below 500 eV is poorer. Figure 3 shows the selected  $K^0$  together with its initial form and  $\lambda * K$  obtained by REELS experiments [7].

#### 4.2 Convergence to the value by TPP

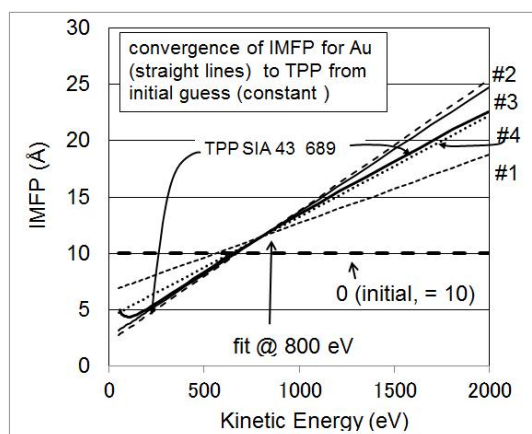


Fig. 4 Convergence of  $\lambda$  to TPP line (bold line) [8]. The arbitrary constant  $c$  is adjusted so that the both values coincide at 800 eV.

Figure 4 shows the estimated  $\lambda$ 's convergence to the TPP line (bold line, denoted as  $\lambda_{TPP}$ ) [8], where the coefficient  $c$  is chosen so that  $c\lambda_0$  coincides with  $\lambda_{TPP}$  at 800 eV. Relative deviations of the thus estimated  $\lambda$  from

$\lambda_{\text{TPP}}, (\lambda - \lambda_{\text{TPP}}) / \lambda_{\text{TPP}}$ , are less than 2.4% in the interval of 700 - 1500 eV KE. The relative peak ratios using this final  $\lambda$  are in good agreement with those predicted by cross sections [4] and asymmetry parameters [5] as shown in Table 2.

## 5. Conclusions

Thus, all the involved parameters and methods, i.e., cross sections, asymmetry parameters, transmission correction procedure, and background optimization, are in an excellent consistency. It is unlikely that this is a mere coincidence. Although the determination of the absolute value of  $\lambda$  was not possible because absolute intensity measurement was not carried out, it should be noted that usual practical surface analysis works on relative intensities only. It is also noted that an analysis without using asymmetry factors will be possible only if the used spectrometer is configured in the magic-angle geometry.

How about the case that  $\lambda$  is not expected to be linear? The present discussion indicates that  $\lambda$ 's at the core peak positions are similarly estimated. In order to interpolate these points, experiment by variable-energy light source would be obviously helpful. In addition, Auger peaks, if any, whose intensities are well understood would be also useful.

Considering that  $J$  and the inelastic background are complementary to each other in the sense that the sum of these two is always equal to the measured intensity, it is

no wonder that the present approach has given the results that are similar to those attained through orthodox bottom-up ones, i.e., those first trying to reproduce the inelastic background from a few basic parameters or other experimental results. This is an example of the existence of an alternative approach to problems that have some challenging and intractable parts with usual methods, i.e., the effort to reproduce  $K^0$  and  $g$  from basic material parameters.

## 6. Acknowledgements

I am grateful to Dr. Akihiro Tanaka for a detailed lecture on the transmission correction procedure of PHI spectrometer. I thank Dr. Shigeo Tanuma for supplying his unpublished data at an early stage of this work.

## 7. References

- [1] M. Jo, *Surf. Interface Anal.* **35**: 729-737 (2003).
- [2] S. Tougaard, *J. Electron Spectrosc. Relat. Phenom* **52**, 243 (1990).
- [3] M. Fukushima, *Math. Program.* **35**, 253 (1986).
- [4] J. H. Scofield, *J. Electron Spectrosc. Relat. Phenom.* **8**, 129, (1976).
- [5] A. Jablonski, *Surf. Interface Anal.* **23**, 29 (1995).
- [6] A. Tanaka, *J. Surf. Anal.* **1**, 189 (1995) (in Japanese).
- [7] S. Tougaard and J. Kraer, *Phys. Rev.* **B43**, 1651 (1991).
- [8] S. Tanuma, C. J. Powell and D. R. Penn, *Surf. Interface Anal.* **43**, 689 (2011).